THE JOURNAL OF BIOLOGICAL CHEMISTRY VOL. 286, NO. 25, pp. 22203–22210, June 24, 2011

Homodimerization of the Src Homology 3 Domain of the Calcium Channel β-Subunit Drives Dynamin-dependent Endocytosis*[S]

Received for publication, November 10, 2010, and in revised form, April 6, 2011 Published, JBC Papers in Press, April 18, 2011, DOI 10.1074/jbc.M110.201871

Erick Miranda-Laferte[‡], Giovanni Gonzalez-Gutierrez[‡1], Silke Schmidt[‡], Andre Zeug[‡], Evgeni G. Ponimaskin[‡], Alan Neely[§], and Patricia Hidalgo[‡2]

From the[‡]Institut für Neurophysiologie, Medizinische Hochschule Hannover, 30625 Hannover, Germany and [§]Centro Interdisciplinario de Neurociencia de Valparaíso, Universidad de Valparaíso, Valparaíso 2349400, Chile

Voltage-dependent calcium channels constitute the main entry pathway for calcium into excitable cells. They are heteromultimers formed by an α_1 pore-forming subunit ($Ca_V\alpha_1$) and accessory subunits. To achieve a precise coordination of calcium signals, the expression and activity of these channels is tightly controlled. The accessory β-subunit ($Ca_V\beta$), a membrane associated guanylate kinase containing one guanylate kinase (β-GK) and one Src homology 3 (β-SH3) domain, has antagonistic effects on calcium currents by regulating different aspects of channel function. Although β-GK binds to a conserved site within the α_1-pore-forming subunit and facilitates channel opening, β-SH3 binds to dynamin and promotes endocytosis. Here, we investigated the molecular switch underlying the functional duality of this modular protein. We show that β-SH3 homodimerizes through a single disulfide bond. Substitution of the only cysteine residue abolishes dimerization and impairs internalization of L-type $Ca_V1.2$ channels expressed in *Xenopus* oocytes while preserving dynamin binding. Covalent linkage of the β-SH3 dimerization-deficient mutant yields a concatamer that binds to dynamin and restores endocytosis. Moreover, using FRET analysis, we show in living cells that $Ca_V\beta$ form oligomers and that this interaction is reduced by $Ca_V\alpha_1$. Association of $Ca_V\beta$ with a polypeptide encoding the binding motif in $Ca_V\alpha_1$ inhibited endocytosis. Together, these findings reveal that β-SH3 dimerization is crucial for endocytosis and suggest that channel activation and internalization are two mutually exclusive functions of $Ca_V\beta$. We propose that a change in the oligomeric state of $Ca_V\beta$ is the functional switch between channel activator and channel internalizer.

Voltage-dependent calcium channels link membrane depolarization to transient increases in cytosolic calcium concentration, which in turn mediate a variety of cellular processes, including gene expression, contraction, neurotransmission, and exocytosis (1). To direct the signal to a specific subset of an extensive family of effectors, cells are endowed with a complex network of regulators that constrain the timing and spreading of the calcium increase. The subset of voltage-dependent calcium channels that are activated by strong depolarization, also called high voltage-activated (HVA)[3] channels, are heteromultimers consisting of a central pore-forming subunit ($Ca_V\alpha_1$) that associates with one or more accessory subunits. Among them the accessory β-subunit ($Ca_V\beta$) has traditionally been recognized as one of the most important modulator of HVA channels (1–3). More recently, it has been shown that the same subunit mediates several other cellular processes (for review, see Ref. 4), including regulation of insulin secretion (5), gene transcription (6) and endocytosis (7). Four $Ca_V\beta$ isoforms ($Ca_V\beta_1$ to $Ca_V\beta_4$) have been cloned from different nonallelic genes. Crystallographic studies of three of these provided the molecular basis for its functional versatility by identifying two protein-protein interactions modules: an Src homology 3 (β-SH3) and a guanylate kinase (β-GK), which are typically found in members of the membrane-associated guanylate kinase family of scaffolding proteins (see Fig. 1*A*) (8–10). The functional multiplicity of $Ca_V\beta$ is achieved by establishing pairwise interactions with other protein partners beside $Ca_V\alpha_1$. How $Ca_V\beta$ sorts out the different molecular targets inside the cell remains elusive. One of these partners is dynamin, the GTPase that scisses newly formed vesicles from the plasma membrane during endocytosis (11, 12). Dynamin contains a proline-rich region with several P*xx*P consensus motifs that serve as docking sites for SH3 domains (13). SH3/proline-rich region-mediated interactions appear to recruit dynamin to areas of endocytosis (14, 15). SH3 domains are small modules found in a variety of proteins that mediate inter- and intramolecular interactions (16). Several conserved amino acids are critical for binding to the P*xx*P motif in the ligand proteins. These residues are also present in the SH3 domain of $Ca_V\beta$, but they appear occluded in the crystal structure (8–10). However,

* This work was supported by grants from the Deutsche Forschungsgemeinschaft Grants DFG Hi 800/3-1 and 4-1 (to P. H.), Red de Anillo de Ciencia y Tecnologia Grant RED-24 (to A. N.), and the German-Chilean Scientific Cooperation Program Deutsche Forschungsgemeinschaft-Comisión Nacional de Investigación Científica y Tecnológica 2010 (to P. H. and A. N.).

[S] The on-line version of this article (available at http://www.jbc.org) contains supplemental Figs. S1–S3, a movie, and additional references.

[1] Present address: Department of Molecular and Integrative Physiology, University of Illinois at Urbana-Champaign, Urbana, IL 61801.

[2] To whom correspondence should be addressed: Medizinische Hochschule Hannover, Institut für Neurophysiologie, Carl-Neuberg-Strasse 1, 30625 Hannover, Germany. Tel.: 49-511/532-2883; Fax: 49-511/532-2776. E-mail: hidalgo.patricia@mh-hannover.de.

[3] The abbreviations used are: HVA, high voltage-activated channel(s); $Ca_V\alpha_1$, α_1 pore-forming subunit of HVA channel(s); $Ca_V\beta$, accessory β-subunit of HVA channel(s); SH3, Src homology 3; GK, guanylate kinase; AID, α_1-interaction domain; BN-PAGE, blue native PAGE; CMBI, charge-movement based internalization; Ef_D, apparent FRET efficiency; CFP, Cyan Fluorescent Protein; pC, pico Coulomb.

the β-SH3 domain does bind to dynamin (7), suggesting that the P*xx*P binding motif becomes exposed by a yet to be discovered regulatory event. Furthermore, following association of the SH3 domain of $Ca_V\beta$ with dynamin, the number of channels at the plasma membrane is reduced (7). Conversely, association of the GK domain of $Ca_V\beta$ with a highly conserved binding motif in $Ca_V\alpha_1$, known as the α_1-interaction domain (AID) (17) favors the coupling between voltage and channel opening in HVA channels (see Fig. 1*A*) (18). Although much has been speculated over the mechanism by which $Ca_V\beta$ alters the open probability of the channel (19–21), how this protein is rerouted to the endocytic pathway has not yet been explored.

Several canonical SH3-containing proteins form dimers to accomplish a particular function (22–24). Amphysisin, the major binding partner of dynamin in mammalian brain, forms heterodimers between two similar isoforms to recruit dynamin to clathrin-coated pits in nerve terminals (22). The islet-brain 1 scaffold protein and CT10 regulator of kinase-like adaptor protein are examples in which homodimerization appears to be involved in regulation of function (23, 24). Here, we investigated the oligomeric state of β-SH3 and show that dimerization of β-SH3 engages $Ca_V\beta$ toward the endocytic pathway.

EXPERIMENTAL PROCEDURES

cDNA Constructs and Recombinant Proteins—The $Ca_V1.2$ channel construct and dynamin has been described elsewhere (7). Full-length $Ca_V\beta_{2a}$ (Swiss-Prot entry Q8VGC3), β-SH3, and β-SH3 C113A monomer and concatamer versions were prepared as described (7, 25). All recombinant protein constructs bear a His_6 tag fused at the N-terminal end of the protein. GST alone and GST fused to the intracellular loop encompassing the AID site from $Ca_V2.3$, hereby referred as to GST-AID, were produced as described previously (25).

Pulldown Assays—Pulldown assays with His-tagged β-SH3 derivatives were performed as described (7). Cobalt-based agarose beads were coupled to the proteins and incubated with pre-cleared extract from tsA201 cells transfected with a dynamin-encoding plasmid 24 to 36 h earlier. Bound proteins were eluted with SDS-PAGE loading buffer and resolved on SDS-PAGE. Immunoblot analysis was done using anti-dynamin antibody (BD Biosciences).

Xenopus Oocyte Preparation, Injection, and Electrophysiological Recordings—*Xenopus laevis* oocytes were prepared, injected, and maintained as in a previous report (26). Electrophysiological recordings on $Ca_V1.2$-expressing oocytes were performed using the cut-open oocyte technique with a CA-1B amplifier (Dagan Corp., Minneapolis MN) as described (25). Gating currents were separated from ionic currents by stepping the membrane voltage near the reversal potential for the permeant ion (Ba^{2+}) (7). Data acquisition and analysis were performed using the pCLAMP system and software (Axon Instruments Inc., Foster City, CA). Currents were filtered at 2 kHz and digitized at 10 kHz. Linear components were eliminated by P/-4 prepulse protocol that consisted of four consecutives pulses a fourth of the amplitude of the test pulse. Current traces during these prepulses were added together and substracted from the current traces obtained with the main pulse.

FRET Analysis—$Ca_V\beta_2$ was fused at its carboxyl-terminal end to either YFP ($Ca_V\beta$-YFP) or CFP ($Ca_V\beta$-CFP) by standard PCR methods. Mammalian tsA201 cells grown on coverslips (15-mm diameter) were co-transfected with YFP- and CFP-tagged $Ca_V\beta_2$-encoding plasmids using Lipofectamine™ (Invitrogen). Spectral analysis of living tsA210 cells co-expressing CFP- and YFP-tagged $Ca_V\beta_2$ constructs were performed according to Kobe *et al.* (27). Quantitative linear unmixing FRET (lux-FRET) analysis in cuvettes and at the single cell level were performed 18–24 h after transfection as described recently (28, 29). Lux-FRET allows determination of FRET efficiencies of donor-acceptor pairs in the presence of free donor and acceptor molecules.

Blue Native (BN)-PAGE—BN-PAGE was done as described (30). Briefly, proteins were incubated for 30 min at room temperature with loading buffer alone or supplemented with either 10 mM DTT, 1% SDS, or both. Proteins were resolved in a gradient polyacrylamide gel (4–25%) overnight at 4 °C using cathode buffer containing 100 mM histidine, 0.002% Serva Blue G powder (SERVA electrophoresis), pH 8.0, and anode buffer containing 100 mM Tris, pH 8.8.

RESULTS

β-SH3 Dimerizes through a Single Disulfide Bond—Here, we studied the quaternary structure of β-SH3 by BN-PAGE that is particularly suited to analyze the oligomeric structure of proteins (31–34). The first hint that β-SH3 forms dimers came from size-exclusion chromatography of isolated β-SH3 indicating some degree of dimerization (35) and from non-reducing SDS-denaturing PAGE showing a small fraction resistant to denaturation (supplemental Fig. 1). In BN-PAGE, β-SH3 migrates in two bands, suggesting the co-existence of two oligomeric states (Fig. 1*B*). Incubation with SDS resulted in no significant changes in the mobility or relative intensity of both bands. In contrast, treatment with the reducing agent DTT causes the disappearance of the upper band, suggesting that this oligomer is generated by disulfide bonding. Because the mobility of the protein in non-denaturing electrophoresis depends on the shape, the numbers of monomers assembled per protein complex cannot be readily determined. To address this issue, we engineered a concatenated cDNA construct by linking two β-SH3 coding regions in a single open reading frame to yield a concatameric β-SH3 protein. This concatamer eluted from a size-exclusion column slightly earlier than its monomeric counterpart and was resolved at the expected molecular mass by reducing SDS-PAGE (Fig. 1*C*). In BN-PAGE, the upper band of the non-covalently linked β-SH3 migrated at the same position as the concatamer, demonstrating that it corresponds to a dimeric form and, accordingly, the lower molecular band to the monomeric form.

To further assess the contribution of disulfide bonding to dimer formation, we substituted the single cysteine residue in β-SH3, located at position 113, by alanine (β-SH3 C113A) and followed the same expression and purification methodology developed for wild-type β-SH3 (7). β-SH3 C113A elutes as a monodisperse peak from a size-exclusion column at the same position as wild-type β-SH3 (Fig. 1*C*), but in BN-PAGE, it migrates as a single band faster than the β-SH3 concatamer

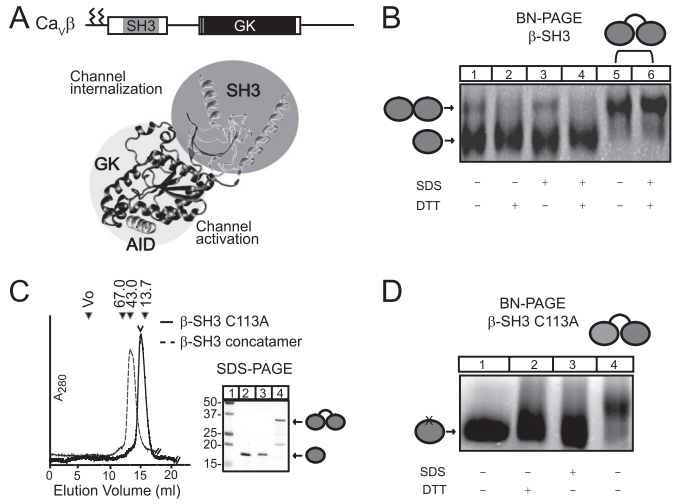

FIGURE 1. **Wild-type β-SH3 domain but not β-SH3 C113A forms dimers.** *A*, schematic and ribbon representation of $Ca_V\beta$ structure in complex with the highly conserved β-binding site of $Ca_V\alpha_1$ (*AID*, helix shown in *gray*) (Protein Data Bank code 1TOJ). SH3, shown in *gray*, and GK, shown in *black*, modulate different channel functions. The two N-terminal cysteine residues that undergo palmitoylation in $Ca_V\beta_{2a}$ variant used in this study are marked by *zigzag lines* in the sketch at the *top* of the *panel*. *B*, oligomeric state of wild-type β-SH3 determined by BN-PAGE. *Lanes 1–4* were loaded with β-SH3, and *lanes 5* and *6* were loaded with β-SH3 concatamer. To induce dissociation into lower-order oligomeric states, including monomers, samples were treated as indicated at the bottom of the panel as described under "Experimental Procedures." *C*, size-exclusion chromatography profile (Superdex 200 10/30 column, GE Healthcare) of β-SH3 C113A and β-SH3 concatamer. The corresponding profile for wild-type β-SH3 has been shown elsewhere (7), and its peak, corresponding to the monomeric fraction, is denoted here with an *open arrowhead*. The elution volume of molecular weight standards are indicated above the chromatogram. *Numbers* correspond to molecular masses in kDa. *Vo*, void, 67.0 (albumin); 43.0 (ovalbumin); and 13.7 (ribonuclease). The *adjacent panel* shows the same proteins resolved onto a reducing SDS-PAGE: *lane 1*, molecular weight standards; *lane 2*, wild-type β-SH3; *lane 3*, β-SH3 C113A; and *lane 4*, β-SH3 concatamer. *D*, oligomeric state of β-SH3 C113A determined by BN-PAGE. *Lanes 1–3* were loaded with β-SH3 C113A, and *lane 4* was loaded with β-SH3 concatamer. Samples were treated as indicated.

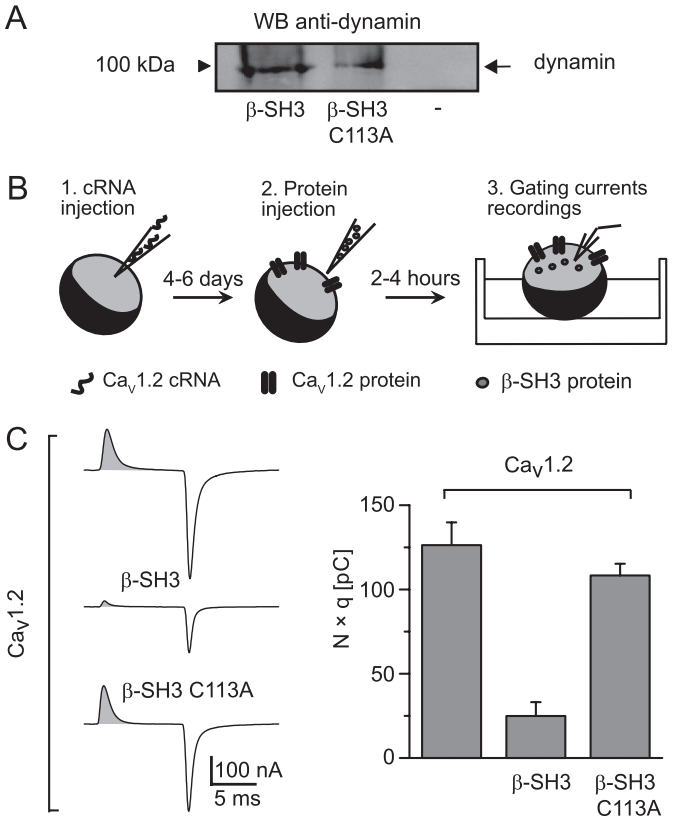

FIGURE 2. **β-SH3 C113A dimerization-deficient mutant preserves its association with dynamin but loses the endocytic capability.** *A*, Western blot of a pull-down assay using His-tagged wild-type and C113A β-SH3 as bait. Lysates from cells expressing dynamin were incubated with either β-SH3 (*lane 1*) or β-SH3 C113A (*lane 2*) precoupled to cobalt beads or with cobalt beads alone (*lane 3*). Bound proteins were detected with anti-dynamin antibody. *B*, a schematic describing the experimental protocol for CMBI assay. *1*, *Xenopus* oocytes are first injected with $Ca_V\alpha_1$-encoding cRNA; *2*, after a few days, when the channels are already expressed at the plasma membrane, oocytes are reinjected with the test protein; and *3*, a few hours later, gating currents are recorded. *C*, representative gating currents recordings and CMBI assay results from *Xenopus* oocytes expressing $Ca_V1.2$ alone and following injection of either β-SH3 or β-SH3 C113A. The *shaded area* under the gating current represents the total amount of charges moved during the voltage step and equals the number of channels (N) times the number of charges displaced per channel (*q*). The bar graph shows N × *q* values from oocytes expressing the indicated channel-protein combinations; $Ca_V1.2$ alone (120 ± 13 pC, $n = 14$), $Ca_V1.2$+β-SH3 (25 ± 8 pC, $n = 12$), and $Ca_V1.2$+β-SH3 C113A (108 ± 7 pC, $n = 17$). Average N × *q* values of $Ca_V1.2$+β-SH3 oocytes were significantly smaller that for $Ca_V1.2$ alone ($p < 2.0 \times 10^{-6}$) or $Ca_V1.2$+β-SH3 C113A ($p < 1.3 \times 10^{-8}$) according to a two-tailed *t* test.

(Fig. 1*D*). This migration pattern was not altered by treatment with either SDS or DTT demonstrating that β-SH3 C113A does not form dimers. We conclude that wild-type β-SH3 forms homodimers bound covalently through a single disulfide bond involving cysteine residue 113.

β-SH3 C113A Dimerization-deficient Mutant Associates with Dynamin but Does Not Promote Endocytosis—We next examined whether the dimeric quaternary structure of β-SH3 plays a role in regulating endocytosis. In a standard pulldown assay, His-tagged wild-type and C113A β-SH3 used as bait brought down dynamin expressed in tsA201 cells (Fig. 2*A*). Thus, eliminating dimer-forming cysteine 113 did not prevent association with dynamin but, as revealed by charge-movement based internalization (CMBI) assay, it abolished the capability to promote endocytosis. The CMBI assay relies on the recording of the so-called gating currents from voltage-activated ion channels expressed in *Xenopus* oocytes (Fig. 2*B*). Gating currents arise from the displacement across the membrane of highly conserved basic residues within the voltage sensor of these channels at the onset of a voltage step (36). When recorded at the ionic current reversal potential, gating currents are void of contamination by ionic currents, and their integral equals the number of channels (N) times the number of charges displaced per channel (*q*) that is constant for each type of channel (37). Other methods to estimate the number of channels such as immunodetection of extracellularly epitope-tagged channels correlates well with CMBI measurements but do not allow simultaneous assessment of channel function (25). Fig. 2*C* shows the results of CMBI assay using the $Ca_V1.2$ isoform of $Ca_V\alpha_1$ before and after the injection of either wild-type β-SH3 or β-SH3 C113A. Although β-SH3 effectively reduces the number of channels in the plasma membrane, the C113A dimerization-deficient mutant does not, despite being capable of associating with dynamin. Thus, dimerization appears crucial to engage β-SH3 in the endocytic pathway.

Covalently Linking Two β-SH3 C113A Dimerization-deficient Mutant Molecules Restores Endocytosis—The observation that the β-SH3 C113A dimerization-deficient mutant binds dynamin but does not internalize channels predicts that bring-

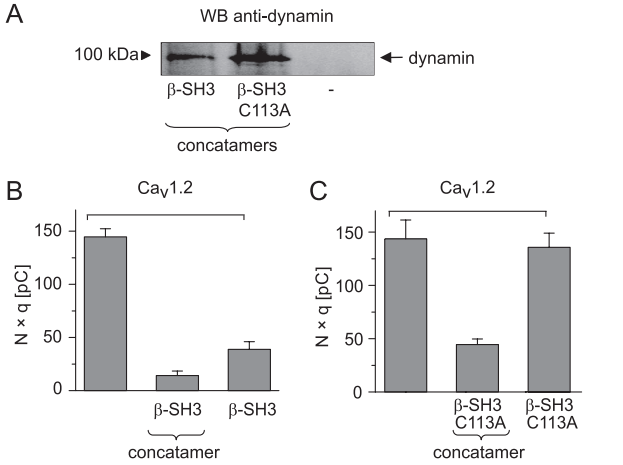

FIGURE 3. **Covalently linking two molecules of β-SH3 C113A dimerization-deficient mutant restores the endocytic capability.** *A*, Western blot (*WB*) of a pulldown assay was done as described in the legend to Fig. 2 but instead used concatameric versions of β-SH3 and β-SH3 C113A. Lysate from cells expressing dynamin were incubated with either β-SH3 concatamer (*lane 1*) or β-SH3 C113A concatamer (*lane 2*) or with cobalt beads alone (*lane 3*). *B*, CMBI assay results from *Xenopus* oocytes expressing $Ca_V1.2$ alone and in combination with β-SH3 either as a concatamer or non-covalently linked. The bar graph shows N × *q* values from oocytes expressing the indicated channel-protein combinations; $Ca_V1.2$ alone (145. ± 8 pC, $n = 9$), $Ca_V1.2$+β-SH3 concatamer (15 ± 4 pC, $n = 6$), and $Ca_V1.2$+β-SH3 (39 ± 7 pC, $n = 8$). Average N × *q* values were significantly smaller in the presence of β-SH3 ($p < 5.7 \times 10^{-9}$) or β-SH3 concatamer ($p < 2.4 \times 10^{-8}$) compared with $Ca_V1.2$ alone. Values for N × *q* between monomer and concatamers were also different but to a smaller degree ($p < 0.04$). *C*, same as *B*, but from *Xenopus* oocytes expressing $Ca_V1.2$ alone and in combination with either a β-SH3 C113A concatamer or β-SH3 C113A. The bar graph shows average N × *q* values for the indicated channel-protein combinations; $Ca_V1.2$ alone (143 ± 18 pC, $n = 11$), $Ca_V1.2$+β-SH3 C113A concatamer (44 ± 5 pC, $n = 9$), or $Ca_V1.2$+β-SH3 C113A (136 ± 13 pC, $n = 15$). Average N × *q* values were significantly smaller for $Ca_V1.2$+β-SH3 C113A concatamer than for $Ca_V1.2$ alone ($p < 4.2 \times 10^{-6}$) or $Ca_V1.2$+β-SH3 C113A ($p < 2.9 \times 10^{-5}$) according to a two-tailed *t* test.

ing together two β-SH3 C113A molecules will rescue endocytosis. We engineered a concatamer β-SH3 C113A and compared it with the wild-type β-SH3 concatamer. Both concatamers eluted from a size-exclusion column at the same position (supplemental Fig. 2), and both retained the ability to associate with dynamin (Fig. 3*A*). The dimerization-competent molecules joined in a single polypeptide chain also retained the endocytic phenotype of the non-covalently linked β-SH3 (Fig. 3*B*), indicating that the molecular linkage did not introduce major structural rearrangements. More remarkably, linking two molecules of the dimerization-deficient mutant indeed restored β-SH3 ability to internalize $Ca_V1.2$ channels (Fig. 3*C*). This result highlights the functional relevance of β-SH3 dimerization for endocytosis.

Membrane-targeted $Ca_V\beta_{2a}$ Isoform Forms Dimers—We have shown previously that when association with $Ca_V\alpha_1$ is prevented, $Ca_V\beta_{2a}$ is as potent as the SH3 domain alone in downregulating HVA channels (7). $Ca_V\beta_{2a}$ is a unique variant of $Ca_V\beta$ that undergoes dynamic palmitoylation (see Fig. 1*A*), and it is targeted to the plasma membrane even in the absence of the $Ca_V\alpha_1$ pore-forming subunit (38, 39). To investigate intermolecular interactions within $Ca_V\beta$, we examined FRET occurrence between fluorophore-labeled $Ca_V\beta_{2a}$ in living cells. Fluorophores CFP and YFP were fused to the C terminus to yield $Ca_V\beta_{2a}$-CFP and $Ca_V\beta_{2a}$-YFP, respectively. Fig. 4*A* shows the fluorescence emission spectra measured in a cuvette containing cells transfected with $Ca_V\beta_{2a}$-CFP and $Ca_V\beta_{2a}$-YFP encoding plasmid together or separately. Only cells coexpressing $Ca_V\beta_{2a}$-CFP and $Ca_V\beta_{2a}$-YFP demonstrated a larger emission peak at 525 nm concomitant with a smaller CFP emission that reflects the energy transferred from the donor CFP to the acceptor YFP. These results indicate that $Ca_V\beta_{2a}$ oligomerizes within living cells. To calculate the apparent FRET efficiency (Ef_D) we applied the lux-FRET approach (28) and found that Ef_D was 10 ± 1% in co-transfected cells, whereas this value was 0 ± 1% in the mix of single transfected cells. Combination of FRET analysis with confocal microscopy revealed that $Ca_V\beta_{2a}$-CFP and $Ca_V\beta_{2a}$-YFP are localized almost entirely at the plasma membrane and that membrane-anchored $Ca_V\beta_{2a}$ showed the highest Ef_D (10.8 ± 1.5%), whereas FRET value measured in minor cytosolic fraction of $Ca_V\beta_{2a}$ (1.7 ± 0.4%) was close to that obtained for negative control (0 ± 0.4%) (Fig. 4*B* and supplemental Movie). Fusing the fluorescence proteins to the N-terminal end of $Ca_V\beta_{2a}$ drastically change its intracellular localization from membrane-bound to homogenously distributed throughout the entire cell.

YFP and CFP proteins linked together in a single polypeptide chain (tandem construct) yields an Ef_D ~35% when measured under the same experimental conditions. This value sets an upper limit of 17.5% to Ef_D in co-transfected cells as only 50% of the β-subunit dimers carry the YFP-CFP pair, the remaining fraction composed of YFP-YFP and CFP-CFP complexes are not detectable by FRET. Thus, the Ef_D of 10% obtained in the present study indicates that in intact cells an important fraction of $Ca_V\beta_{2a}$ oligomerizes.

In BN-PAGE, $Ca_V\beta_{2a}$ display a migration pattern consistent with dimer formation as it compares to the one obtained with a concatenated $Ca_V\beta$ protein construct (Fig. 4*C*). The $Ca_V\beta_{2a}$ concatamer shows an additional band that corresponds to monomeric $Ca_V\beta$ likely produced by proteolysis (supplemental Fig. 3) (40). In contrast to β-SH3, $Ca_V\beta_{2a}$ dimers were resistant to incubation with either SDS or DTT and could only be disrupted by treatment with both agents (Fig. 4*C*). Substitution of C113 by alanine ($Ca_V\beta_{2a}$ C113A) did not prevent dimer formation (Fig. 4*D*), indicating that other regions of the full-length protein contribute to the dimerization interface. This idea is supported by our earlier experiments demonstrating that isolated GK domain forms dimers (18). In addition, a recent report showed higher-order oligomerization in cytosolic $Ca_V\beta$ variants coexpressed with the $Ca_V\alpha_1$ pore-forming subunit that depends on specific sites within the GK domain (41). From our experiments, the existence of less stable higher organized oligomeric forms of $Ca_V\beta_{2a}$ cannot be excluded.

Preassociation of $Ca_V\beta_{2a}$ with a Polypeptide Encoding Binding Motif of α_1 Pore-forming AID Inhibits Endocytosis—We have shown previously that full-length $Ca_V\beta_{2a}$ is as efficient as the SH3 domain to promote endocytosis of $Ca_V\alpha_1$ when association to it is prevented and that it also induces internalization of the distantly related *Shaker* potassium channel (7). Deletion of the highly conserved AID sequence located in the intracellular loop joining the first and second domain of $Ca_V1.2$ ($Ca_V1.2$ ΔAID) effectively disrupts any $Ca_V\beta$-$Ca_V\alpha_1$ association. Here, we used the same strategy to follow endocytosis mediated by $Ca_V\beta_{2a}$. $Ca_V1.2$ ΔAID channels were internalized by $Ca_V\beta_{2a}$

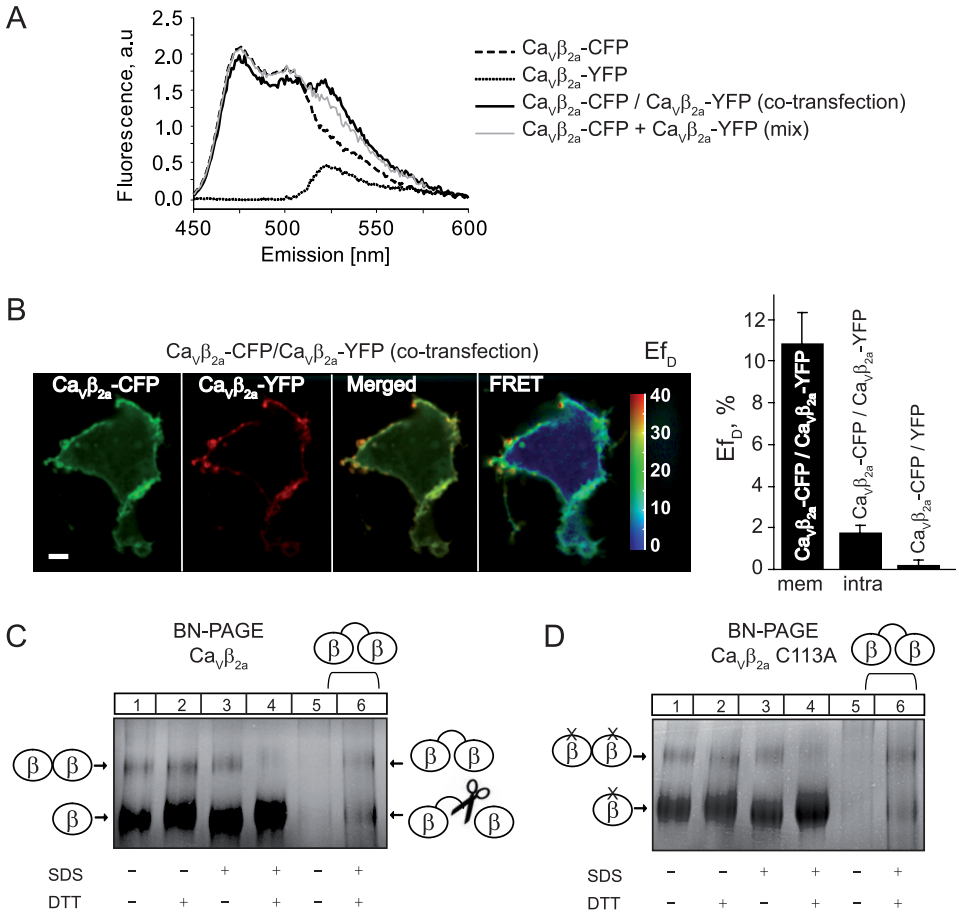

FIGURE 4. **Membrane-targeted Ca$_V$β$_{2a}$ also forms dimers.** *A*, fluorescence emission spectra of living tsA210 cells expressing the indicated CFP- and YFP-tagged Ca$_V$β$_{2a}$ constructs either separately or together (co-transfection). Mix corresponds to the emission spectra of a mixture of single transfected cells (*mix*). Emission spectra were collected at excitation wavelength λ_{exc} = 440 nm. *a.u.*, arbitrary units. *B*, distribution and quantitative pixel-based FRET analysis of CFP-and YFP-tagged Ca$_V$β$_{2a}$ in living tsA210 cells. *Scale bar*, 5 μm. Ef$_D$, apparent FRET efficiency, *mem*, membrane-localized Ca$_V$β$_{2a}$; *intra*, intracellular-localized Ca$_V$β$_{2a}$. Data represent mean values ± S.E. (n = 6). *C*, BN-PAGE analysis of Ca$_V$β$_{2a}$. *Lanes 1–4* were loaded with Ca$_V$β$_{2a}$ and *lanes 5* and *6* with the Ca$_V$β$_{2a}$ concatamer. In the absence of SDS, the Ca$_V$β$_{2a}$ concatamer is poorly resolved (*lane 5*). Samples were treated as indicated at the *bottom* of the *panel*. *D*, BN-PAGE analysis of Ca$_V$β$_{2a}$ C113A. *Lanes 1–4* were loaded with Ca$_V$β$_{2a}$ C113A and *lanes 5* and *6* were loaded with the Ca$_V$β$_{2a}$ concatamer.

wild-type as well as by the C113A mutant. This result emphasizes that dimer formation rather than the chemical nature of the residue at this position is critical for endocytosis (Fig. 5*A*). The fact that Ca$_V$β$_{2a}$ efficiently internalizes channels lacking the AID site suggests that its association with the pore-forming subunit hinders channel internalization. To test this idea, we preincubated Ca$_V$β$_{2a}$ with GST-AID, a GST-fusion protein that included the AID sequence, and performed CMBI assay. Association of Ca$_V$β$_{2a}$ with the AID site inhibited endocytosis (Fig. 5*B*). These findings are consistent with a model whereby channel activation and internalization are mutually exclusive functions of Ca$_V$β.

α$_1$ Pore-forming Subunit Impairs Dimer Formation of Ca$_V$β$_{2a}$—Because it is well established that only one β-subunit is required to recapitulate channel function, it is likely that association with Ca$_V$α$_1$ disrupts dimerization. The latter would explain why co-incubation with the AID channel peptide inhibits endocytosis (Fig. 5*B*) and also why we did not observe β-mediated endocytosis in the wild-type channel but did observe it in channels lacking the AID site (7). We performed the same FRET analysis shown in Fig. 4*A* but this time in the presence of Ca$_V$1.2. We observed a decrease in Ef$_D$ of almost 50% when fluorescently labeled Ca$_V$β$_{2a}$ proteins are coexpressed together with the α$_1$ pore-forming subunit (Fig. 5*C*).

DISCUSSION

It is increasingly evident that SH3-containing proteins expand their functional diversity by dimerization. For example, in islet brain 1 protein, mutations that destabilize dimer formation do not affect binding with the proline-rich region containing partner c-Jun N-terminal kinase but impairs its ability to regulate insulin secretion (23). In the case of CT10 regulator of kinase-like adaptor protein, a functionally relevant nuclear export signal becomes available only after a conformational change induced by homodimerization (24). Dimerization of β-SH3 could position two dynamin molecules together promoting its oligomerization and GTPase activity (42) or could bring dynamin close to other proteins of the endocytic machinery, serving as a local adaptor that recruits an active endocytic complex. This idea is supported by the observation that two β-SH3 modules brought together by either a disulfide bond or by a covalently attached peptide linker are equally competent for activation of endocytosis. Thus, closeness of the two SH3 domains appears sufficient for function as opposed to the

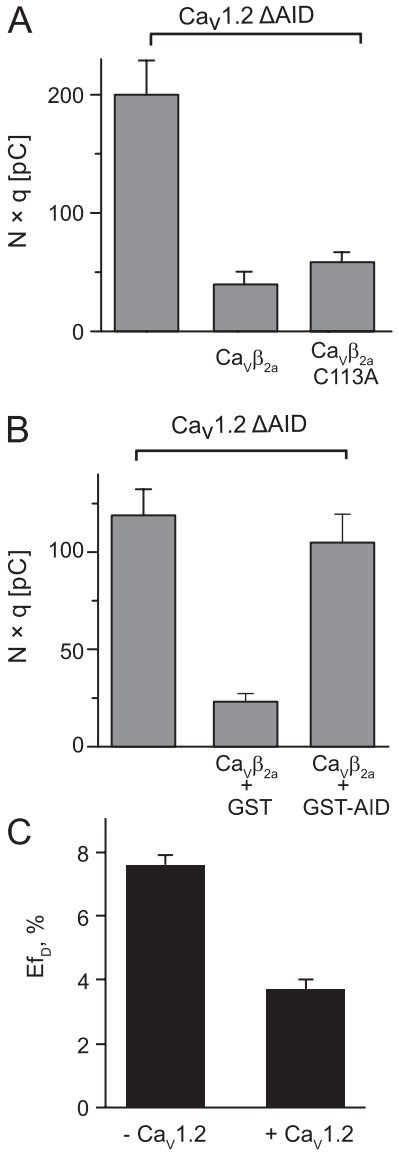

FIGURE 5. **Association of $Ca_V\beta_{2a}$ with the AID motif abolishes channel internalization and impairs dimerization.** *A*, bar graph showing average N × *q* values for the indicated channel-protein combinations. $Ca_V1.2$ ΔAID alone (200 ± 29 pC, $n = 14$) was significantly larger than following injection of either $Ca_V\beta_{2a}$ wild-type (40 ± 11 pC, $n = 8$) or C113A mutant (58 ± 9 pC, $n = 18$). *B*, bar graph showing average N × *q* values for the following: $Ca_V1.2$ ΔAID alone (119 ± 13 pC, $n = 16$) and after injection of $Ca_V\beta_{2a}$ either preincubated with GST (23 ± 4 pC, $n = 11$) or with GST-AID (104 ± 15 pC, $n = 17$). *C*, FRET efficiencies for $Ca_V\beta_{2a}$-CFP and $Ca_V\beta_{2a}$-YFP proteins coexpressed in the absence (7.6 ± 0.3%) and presence (3.7 ± 0.3%) of α_1 pore-forming subunit. FRET experiments were repeated three times with consistent results.

requirement of a precise geometry of the two dynamin binding sites within the quaternary structure of the dimer. Possible candidates to be recruited are members of the Ras superfamily of monomeric small GTPases known to inhibit $Ca_V1.2$-mediated currents by interacting with $Ca_V\beta$ subunits (43). Furthermore, the effect of the Ras protein REM involves dynamin-dependent endocytosis (44), suggesting that REM and dynamin may simultaneously interact with the $Ca_V\beta$ dimer to inhibit calcium currents. The repertoire of regulatory inputs to the endocytic machinery may be augmented even further in full-length $Ca_V\beta$ by the GK domain, which also appears as a protein-protein interaction domain (45–47). Interaction of kinesin-like proteins with GK domains (48) suggests that $Ca_V\beta$ may be engaged in the sorting of the endocytic vesicle by motor proteins. We have already proposed that the functional duality of $Ca_V\beta$ constitutes an efficient quality control mechanism in which the same protein ensures functional fitness and survival of the channel in the plasma membrane (7). In this context, it appears natural to think that channels internalized by $Ca_V\beta$ are directed to early endosomes for recycling rather than to lysosomes for degradation.

Our results hint to a mutual exclusion between channel activation and internalization by $Ca_V\beta$. Whether this functional divergence correlates with $Ca_V\beta$ ability to form dimers when associated to $Ca_V\alpha_1$ remains controversial. Although it is well established that a single $Ca_V\beta$ molecule or β-GK alone fully reconstitutes modulation of HVA channels (18, 49), a recent report suggests that $Ca_V\beta$ oligomers can also bind to the channel and augment current density (41). The authors attributed this current increase to changes in the functional properties of the channels that they correlate to $Ca_V\beta_3$ oligomerization induced by a β-GK fragment. Alternative scenarios are that additional monomeric $Ca_V\beta_3$ increases the fraction of the $Ca_V1.2$ subunit complexed with β-subunit or recruits $Ca_V\alpha_1$-$Ca_V\beta$ channel complexes to the plasma membrane, both augmenting current density (49). Unfortunately, the lack of quantification of the number of channels in the plasma membrane does not allow unambiguous distinction between alterations in channel function or expression.

The number of binding partners and functions of $Ca_V\beta$ is rapidly increasing (4, 50). Very distantly related proteins have been shown to associate with $Ca_V\beta$, including Rem, Rad, kir/Gem (RGK) GTPases, Ahnak, RIM1, bestrophin, heterochromatin protein 1, a yet to be identified member of intracellular calcium stores, and dynamin. Although the exact sequence of events for the switch between $Ca_V\alpha_1$-$Ca_V\beta$ channel to the $(Ca_V\beta)_2$-dynamin complex and the physiological signal that triggers dissociation of the β-subunit from its traditional $Ca_V\alpha_1$ partner have yet to be established, we do know that α_1-β interaction is indeed reversible (25). This fact by itself predicts the presence of free β-subunit that can then interact with other ligands besides $Ca_V\alpha_1$.

In promiscuous proteins, specific associations are often regulated by their structural flexibility. This type of regulation is well documented for the classical members of the membrane-associated guanylate kinase family in which association of ligands with other regions of the molecule regulates GK binding (51–55). The proposed mechanism is that ligands influence SH3-GK intramolecular interactions producing a conformational change within the GK domain that changes the affinity for its partners. For example, upon binding to calmodulin, the synapse-associated protein SAP97 weakens the SH3-GK interaction allowing the accessibility of GK by other proteins (56). Similarly, the SH3-GK interaction that also exists in the β-protein (57–59) may be favored by binding with high affinity to the α_1-subunit. Thus, when complexed with the channel, $Ca_V\beta$ intramolecular interactions dominate over intermolecular associations. This is consistent with the FRET analysis showing that dimer formation of $Ca_V\beta$ is reduced in the presence of the α_1-subunit. On the contrary, by binding to the SH3 domain,

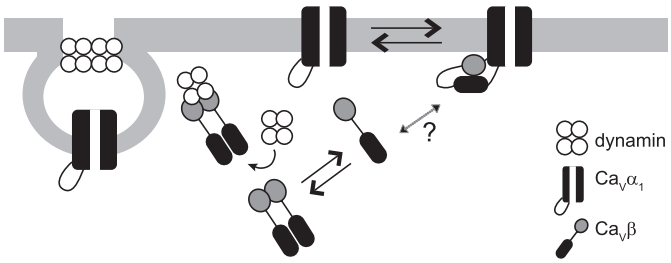

FIGURE 6. **Schematic representation of channel activation and channel internalization by $Ca_V\beta$.** The model illustrates that two different oligomeric states of the protein fulfils two opposing effects on calcium currents. $Ca_V\beta$ binds as a monomer to the AID site of $Ca_V\alpha_1$ through the GK domain (shown in *black*) and activates calcium currents. Dissociation of $Ca_V\beta$ weakens intramolecular SH3-GK interactions, making both domains available for further interactions, including dimerization. Association of $Ca_V\beta$ dimers with dynamin, via its SH3 domain (shown in *gray*), promotes internalization of the channel complex and inhibition of calcium currents through $Ca_V\alpha_1$. It remains to be determined what triggers dissociation of the β-subunit from its traditional $Ca_V\alpha_1$ partner. Other ligand proteins may promote the interaction of $Ca_V\beta$ with dynamin.

dynamin could weaken intramolecular interactions and favors dimer formation and dissociation from the channel. Our study suggests that dimerization contributes to the functional versatility of $Ca_V\beta$ and represents the switch from channel activator to channel internalizer (Fig. 6). Dimerization would endow $Ca_V\beta$ with an additional handle to expand the dynamic range over which this protein controls the spatio-temporal profile of calcium signals. After all, the modular architecture of $Ca_V\beta$ appears very well suited to orchestrate calcium signaling.

One point that needs to be addressed directly is whether dynamin bind to $Ca_V\beta$ when it is complexed to the α_1-subunit. It would be also interesting to know whether post-translational modifications regulate SH3/GK interactions (60).

The existence of multiple pathways in the regulation of calcium currents by $Ca_V\beta$ imposes new theoretical considerations for therapy design. Several evidences suggest that alterations in $Ca_V\beta_2$ underlie some forms of myocardial dysfunction (61–64), and so far, gene therapy to inhibit $Ca_V\beta_2$ has been considered only in correlation to an electrophysiological phenotype (65).

Acknowledgments—We thank Dr. Christoph Fahlke for insightful discussion and Rodrigo Neely for reading the manuscript.

REFERENCES

1. Catterall, W. A. (2000) *Annu. Rev. Cell Dev. Biol.* **16,** 521–555
2. Arikkath, J., and Campbell, K. P. (2003) *Curr. Opin. Neurobiol.* **13,** 298–307
3. Dolphin, A. C. (2003) *J. Bioenerg. Biomembr.* **35,** 599–620
4. Hidalgo, P., and Neely, A. (2007) *Cell Calcium* **42,** 389–396
5. Berggren, P. O., Yang, S. N., Murakami, M., Efanov, A. M., Uhles, S., Köhler, M., Moede, T., Fernström, A., Appelskog, I. B., Aspinwall, C. A., Zaitsev, S. V., Larsson, O., de Vargas, L. M., Fecher-Trost, C., Weissgerber, P., Ludwig, A., Leibiger, B., Juntti-Berggren, L., Barker, C. J., Gromada, J., Freichel, M., Leibiger, I. B., and Flockerzi, V. (2004) *Cell* **119,** 273–284
6. Hibino, H., Pironkova, R., Onwumere, O., Rousset, M., Charnet, P., Hudspeth, A. J., and Lesage, F. (2003) *Proc. Natl. Acad. Sci. U.S.A.* **100,** 307–312
7. Gonzalez-Gutierrez, G., Miranda-Laferte, E., Neely, A., and Hidalgo, P. (2007) *J. Biol. Chem.* **282,** 2156–2162
8. Chen, Y. H., Li, M. H., Zhang, Y., He, L. L., Yamada, Y., Fitzmaurice, A., Shen, Y., Zhang, H., Tong, L., and Yang, J. (2004) *Nature* **429,** 675–680
9. Opatowsky, Y., Chen, C. C., Campbell, K. P., and Hirsch, J. A. (2004) *Neuron* **42,** 387–399
10. Van Petegem, F., Clark, K. A., Chatelain, F. C., and Minor, D. L., Jr. (2004) *Nature* **429,** 671–675
11. Hinshaw, J. E. (2000) *Annu. Rev. Cell Dev. Biol.* **16,** 483–519
12. Praefcke, G. J., and McMahon, H. T. (2004) *Nat. Rev. Mol. Cell Biol.* **5,** 133–147
13. Gout, I., Dhand, R., Hiles, I. D., Fry, M. J., Panayotou, G., Das, P., Truong, O., Totty, N. F., Hsuan, J., Booker, G. W., and. (1993) *Cell* **75,** 25–36
14. David, C., McPherson, P. S., Mundigl, O., and de Camilli, P. (1996) *Proc. Natl. Acad. Sci. U.S.A.* **93,** 331–335
15. Shupliakov, O., Löw, P., Grabs, D., Gad, H., Chen, H., David, C., Takei, K., De Camilli, P., and Brodin, L. (1997) *Science* **276,** 259–263
16. Mayer, B. J. (2001) *J. Cell Sci.* **114,** 1253–1263
17. Pragnell, M., De Waard, M., Mori, Y., Tanabe, T., Snutch, T. P., and Campbell, K. P. (1994) *Nature* **368,** 67–70
18. Gonzalez-Gutierrez, G., Miranda-Laferte, E., Nothmann, D., Schmidt, S., Neely, A., and Hidalgo, P. (2008) *Proc. Natl. Acad. Sci. U.S.A.* **105,** 14198–14203
19. Dzhura, I., and Neely, A. (2003) *Biophys. J.* **85,** 274–289
20. Kanevsky, N., and Dascal, N. (2006) *J. Gen. Physiol.* **128,** 15–36
21. Herzig, S., Khan, I. F., Gründemann, D., Matthes, J., Ludwig, A., Michels, G., Hoppe, U. C., Chaudhuri, D., Schwartz, A., Yue, D. T., and Hullin, R. (2007) *FASEB J.* **21,** 1527–1538
22. Wigge, P., Köhler, K., Vallis, Y., Doyle, C. A., Owen, D., Hunt, S. P., and McMahon, H. T. (1997) *Mol. Biol. Cell* **8,** 2003–2015
23. Kristensen, O., Guenat, S., Dar, I., Allaman-Pillet, N., Abderrahmani, A., Ferdaoussi, M., Roduit, R., Maurer, F., Beckmann, J. S., Kastrup, J. S., Gajhede, M., and Bonny, C. (2006) *EMBO J.* **25,** 785–797
24. Harkiolaki, M., Gilbert, R. J., Jones, E. Y., and Feller, S. M. (2006) *Structure* **14,** 1741–1753
25. Hidalgo, P., Gonzalez-Gutierrez, G., Garcia-Olivares, J., and Neely, A. (2006) *J. Biol. Chem.* **281,** 24104–24110
26. Neely, A., Garcia-Olivares, J., Voswinkel, S., Horstkott, H., and Hidalgo, P. (2004) *J. Biol. Chem.* **279,** 21689–21694
27. Kobe, F., Renner, U., Woehler, A., Wlodarczyk, J., Papusheva, E., Bao, G., Zeug, A., Richter, D. W., Neher, E., and Ponimaskin, E. (2008) *Biochim. Biophys. Acta* **1783,** 1503–1516
28. Wlodarczyk, J., Woehler, A., Kobe, F., Ponimaskin, E., Zeug, A., and Neher, E. (2008) *Biophys. J.* **94,** 986–1000
29. Woehler, A., Wlodarczyk, J., and Ponimaskin, E. G. (2009) *Glycoconj. J.* **26,** 749–756
30. Niepmann, M., and Zheng, J. (2006) *Electrophoresis* **27,** 3949–3951
31. Schägger, H., Cramer, W. A., and von Jagow, G. (1994) *Anal. Biochem.* **217,** 220–230
32. Horiuchi, M., Nicke, A., Gomeza, J., Aschrafi, A., Schmalzing, G., and Betz, H. (2001) *Proc. Natl. Acad. Sci. U.S.A.* **98,** 1448–1453
33. Gendreau, S., Voswinkel, S., Torres-Salazar, D., Lang, N., Heidtmann, H., Detro-Dassen, S., Schmalzing, G., Hidalgo, P., and Fahlke, C. (2004) *J. Biol. Chem.* **279,** 39505–39512
34. Detro-Dassen, S., Schänzler, M., Lauks, H., Martin, I., zu Berstenhorst, S. M., Nothmann, D., Torres-Salazar, D., Hidalgo, P., Schmalzing, G., and Fahlke, C. (2008) *J. Biol. Chem.* **283,** 4177–4188
35. McGee, A. W., Nunziato, D. A., Maltez, J. M., Prehoda, K. E., Pitt, G. S., and Bredt, D. S. (2004) *Neuron* **42,** 89–99
36. Bezanilla, F., and Stefani, E. (1998) *Methods Enzymol.* **293,** 331–352
37. Noceti, F., Baldelli, P., Wei, X., Qin, N., Toro, L., Birnbaumer, L., and Stefani, E. (1996) *J. Gen. Physiol.* **108,** 143–155
38. Chien, A. J., Carr, K. M., Shirokov, R. E., Rios, E., and Hosey, M. M. (1996) *J. Biol. Chem.* **271,** 26465–26468
39. Chien, A. J., Gao, T., Perez-Reyes, E., and Hosey, M. M. (1998) *J. Biol. Chem.* **273,** 23590–23597
40. Nicke, A., Rettinger, J., and Schmalzing, G. (2003) *Mol. Pharmacol.* **63,** 243–252
41. Lao, Q. Z., Kobrinsky, E., Liu, Z., and Soldatov, N. M. (2010) *FASEB J.* **24,** 5013–5023
42. Warnock, D. E., Hinshaw, J. E., and Schmid, S. L. (1996) *J. Biol. Chem.* **271,** 22310–22314

43. Béguin, P., Nagashima, K., Gonoi, T., Shibasaki, T., Takahashi, K., Kashima, Y., Ozaki, N., Geering, K., Iwanaga, T., and Seino, S. (2001) *Nature* **411,** 701–706
44. Yang, T., Xu, X., Kernan, T., Wu, V., and Colecraft, H. M. (2010) *J. Physiol.* **588,** 1665–1681
45. Kim, E., Naisbitt, S., Hsueh, Y. P., Rao, A., Rothschild, A., Craig, A. M., and Sheng, M. (1997) *J. Cell Biol.* **136,** 669–678
46. Takeuchi, M., Hata, Y., Hirao, K., Toyoda, A., Irie, M., and Takai, Y. (1997) *J. Biol. Chem.* **272,** 11943–11951
47. Mathew, D., Gramates, L. S., Packard, M., Thomas, U., Bilder, D., Perrimon, N., Gorczyca, M., and Budnik, V. (2002) *Curr. Biol.* **12,** 531–539
48. Hanada, T., Lin, L., Tibaldi, E. V., Reinherz, E. L., and Chishti, A. H. (2000) *J. Biol. Chem.* **275,** 28774–28784
49. Dalton, S., Takahashi, S. X., Miriyala, J., and Colecraft, H. M. (2005) *J. Physiol.* **567,** 757–769
50. Buraei, Z., and Yang, J. (2010) *Physiol. Rev.* **90,** 1461–1506
51. Brenman, J. E., Topinka, J. R., Cooper, E. C., McGee, A. W., Rosen, J., Milroy, T., Ralston, H. J., and Bredt, D. S. (1998) *J. Neurosci.* **18,** 8805–8813
52. Tavares, G. A., Panepucci, E. H., and Brunger, A. T. (2001) *Mol. Cell* **8,** 1313–1325
53. Qian, Y., and Prehoda, K. E. (2006) *J. Biol. Chem.* **281,** 35757–35763
54. Reese, M. L., Dakoji, S., Bredt, D. S., and Dötsch, V. (2007) *Nat. Struct. Mol. Biol.* **14,** 155–163
55. Newman, R. A., and Prehoda, K. E. (2009) *J. Biol. Chem.* **284,** 12924–12932
56. Paarmann, I., Spangenberg, O., Lavie, A., and Konrad, M. (2002) *J. Biol. Chem.* **277,** 40832–40838
57. Opatowsky, Y., Chomsky-Hecht, O., Kang, M. G., Campbell, K. P., and Hirsch, J. A. (2003) *J. Biol. Chem.* **278,** 52323–52332
58. Takahashi, S. X., Miriyala, J., and Colecraft, H. M. (2004) *Proc. Natl. Acad. Sci. U.S.A.* **101,** 7193–7198
59. Takahashi, S. X., Miriyala, J., Tay, L. H., Yue, D. T., and Colecraft, H. M. (2005) *J. Gen. Physiol.* **126,** 365–377
60. Sabio, G., Arthur, J. S., Kuma, Y., Peggie, M., Carr, J., Murray-Tait, V., Centeno, F., Goedert, M., Morrice, N. A., and Cuenda, A. (2005) *EMBO. J.* **24,** 1134–1145
61. Weissgerber, P., Held, B., Bloch, W., Kaestner, L., Chien, K. R., Fleischmann, B. K., Lipp, P., Flockerzi, V., and Freichel, M. (2006) *Circ. Res.* **99,** 749–757
62. Hullin, R., Matthes, J., von Vietinghoff, S., Bodi, I., Rubio, M., D'Souza, K., Friedrich Khan, I., Rottländer, D., Hoppe, U. C., Mohacsi, P., Schmitteckert, E., Gilsbach, R., Bünemann, M., Hein, L., Schwartz, A., and Herzig, S. (2007) *PLoS One* **2,** e292
63. Link, S., Meissner, M., Held, B., Beck, A., Weissgerber, P., Freichel, M., and Flockerzi, V. (2009) *J. Biol. Chem.* **284,** 30129–30137
64. Koval, O. M., Guan, X., Wu, Y., Joiner, M. L., Gao, Z., Chen, B., Grumbach, I. M., Luczak, E. D., Colbran, R. J., Song, L. S., Hund, T. J., Mohler, P. J., and Anderson, M. E. (2010) *Proc. Natl. Acad. Sci. U.S.A.* **107,** 4996–5000
65. Cingolani, E., Ramirez Correa, G. A., Kizana, E., Murata, M., Cho, H. C., and Marbán, E. (2007) *Circ. Res.* **101,** 166–175